Progress In Electromagnetics Research M, Vol. 59, 1–7, 2017

Sub-Diffraction Holographic Imaging with Resonant Scatterers

Abhishek Patel and Reza K. Amineh*

Abstract—Imaging with electromagnetic waves has a wide range of applications from remote sensing of earth to concealed weapon detection, among the others. When data are collected in the far-field (imaging distance in the order of one wavelength or larger), linear electromagnetic imaging techniques mainly suffer a fundamental limit in the resolution called "diffraction limit". To overcome this limit, we propose the use of resonant near-field scatterers incorporated in the holographic imaging techniques. These scatterers convert part of the evanescent spectrum in the vicinity of the object to propagating spectrum that is measured by the antenna in the far-field. Here, we study the improvement in the resolution with decreasing the object-scatterer distance. We also investigate the effect of using multiple scatterers along the range and cross-range directions.

1. INTRODUCTION

The well-known "diffraction limit" phenomenon restricts the resolution of conventional linear far-field imaging systems. However, imaging below this limit, i.e., with resolution less than half-wavelength when imaging an electromagnetic source and quarter-wavelength when imaging an object, is essential in many applications such as non-destructive testing of materials, remote sensing, underground imaging,etc.

Many techniques have been proposed so far to overcome the diffraction limit, most of which exploit the evanescent field components in the vicinity of the imaged object (e.g., see [1–4]). These components contain information about the finer details of the electromagnetic field variation. Overcoming the diffraction limit for longer imaging distances is very challenging due to the fast attenuation of the evanescent waves. For instance, an approach has been proposed in [5] for sub-diffraction imaging sources in the far-field. To achieve this, superdirectivity antenna design concepts have been employed to design a well-controlled superoscillatory filter based on the properties of Tschebyscheff polynomials. The filter is applied to the holographic images to achieve resolutions beyond the diffraction limit. However, this approach suffers from huge side-lobe levels associated with the superoscillatory filters. This limits the field of view (image size) for this imaging technique.

Another technique to achieve super-resolution in the far-field is based on the projection of the near-field information to the far-field (e.g., see [6]). To achieve this, scatterers are employed in the near-field zone of the imaged sources, i.e., at a distance D where $D \ll \lambda$, to transform a large portion of the evanescent waves in the close proximity of the imaged source to propagating waves. In [6], these propagating waves that carry both subwavelength and non-subwavelength information are refocused by a phase conjugating lens and a similar configuration of the scatterers placed at a similar distance D from the image line (on the other side of the lens). Fig. 1(a) shows the sub-diffraction imaging configuration proposed in [6].

Here, we propose a simple yet effective technique to perform sub-diffraction imaging. Inspired by the hardware implementation in [6] and the holographic imaging technique in [7], we propose a sub-diffraction holographic imaging technique with the measurement of point-spread function (PSF) of the

Received 23 June 2017, Accepted 12 July 2017, Scheduled 27 July 2017

* Corresponding author: Reza K. Amineh (rkhalaja@nyit.edu).

The authors are with the Department of Electrical and Computer Engineering, New York Institute of Technology, NY 10023, USA.

system. Although we propose using a scatterer in the close proximity of the imaged object as in [6], the image reconstruction is performed via processing instead of the use of hardware components such as phase conjugating lens in [6]. Also, collection of the PSF of the imaging system via the measurement of a small object (the so called calibration object (CO) as in [7]) eliminates the need for providing the incident field and the Green's function for the combination of the antenna and the scatterer in the holographic imaging. This is important since any small and inevitable modeling error in the simulation of the incident field and the Green's function leads to large inaccuracies in the imaging results due to the delicacy of the evanescent waves.

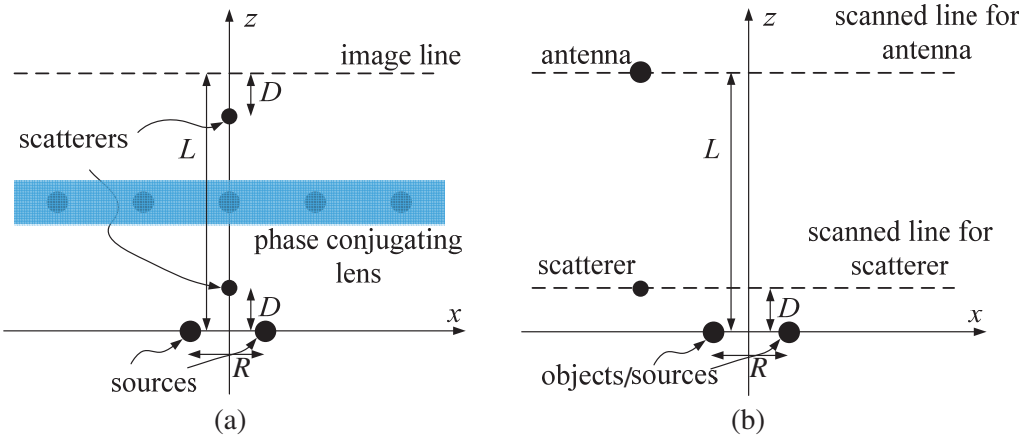

Figure 1. (a) Far-field ($L \geq \lambda$) imaging setup proposed in [6] for sub-diffraction imaging with placing scatterers at a distance D ($D \ll \lambda$) from the imaged sources and image line and also the use of phase conjugating lens. (b) Proposed sub-diffraction imaging setup using near-field scatterers that move together with an antenna scanning in the far-field ($L \geq \lambda$).

2. SUB-DIFFRACTION HOLOGRAPHIC IMAGING

In this section, we first review the principles of holographic imaging with the measurement of PSF of a linear space-invariant imaging system. Then, we propose the use of resonant scatterers to overcome the diffraction limit for the resolution

2.1. Holographic Imaging

In holographic imaging techniques, the scattering model is based on the linear Born approximation. Using this approximation, the integral form of the electromagnetic scattering problem is given by

$$\mathbf{E}^{\mathrm{sc}}(\mathbf{r}_P) \approx \iiint_{V_Q} \left[k_s^2(\mathbf{r}_Q) - k_b^2\right] \mathbf{G}(\mathbf{r}_P, \mathbf{r}_Q) \cdot \mathbf{E}^{\mathrm{inc}}(\mathbf{r}_Q) d\mathbf{r}_Q. \tag{1}$$

Here, $\mathbf{E}^{sc}$ is the scattered field; $\mathbf{G}$ is Green's dyadic function; $\mathbf{E}^{\mathrm{inc}}$ is the incident field; k_s and k_b are the wavenumbers of the object and the background media, respectively; V_Q is the inspected volume. We assume that k_b is known. The position vectors $\mathbf{r}_P$ and $\mathbf{r}_Q$ give the locations of the observation and object's scattering points, respectively.

It has been shown in [7] that PSF of the microwave measurement system (assuming that the imaging system is linear space-invariant) can be approximated by recording the scattered field in (1) through measurement of a small object, termed a calibration object (CO), placed at the same image distance of interest. With reference to Fig. 1(b) (currently we ignore the use of scatterer), the measured scattered field by the antenna over the scanned line for a CO placed at the origin is denoted by $E_j^{\mathrm{sc,co}}(x)$. The measured scattered field by the antenna over the scanned line for any unknown object on $z = 0$ line can

then be approximated as [7]

$$E_j^{\mathrm{sc}}(x') \approx \int_x f(x) \cdot E_j^{\mathrm{sc,co}}(x'-x)dx. \tag{2}$$

where $f(x)$ is the contrast function to be estimated. The scattered fields for the CO and the unknown object in Eq. (2) are obtained by subtracting the measured total field without the presence of any object from the measured total field in the presence of the respective object. Further, the integral over x can be interpreted as a convolution. Thus, the Fourier transform (FT) of $E_j^{\mathrm{sc}}(x')$, $j = x, y, z$, is written as

$$\tilde{E}_j^{\mathrm{sc}}(k_x) \approx \tilde{F}(k_x) \cdot \tilde{E}_j^{\mathrm{sc,co}}(k_x) \tag{3}$$

where $\tilde{F}(k_x)$ and $\tilde{E}_j^{\mathrm{sc,co}}(k_x)$ are the FTs of $f(x)$ and $E_j^{\mathrm{sc,co}}(x)$, respectively, and k_x is the Fourier variable. To reconstruct the contrast function, Equation (3) is solved for $\tilde{F}(k_x)$ directly as

$$\tilde{F}(k_x) \approx \frac{\tilde{E}_j^{\mathrm{sc}}(k_x)}{\tilde{E}_j^{\mathrm{sc,co}}(k_x)} \tag{4}$$

Then, by taking the inverse FT of $\tilde{F}(k_x)$, the estimated contrast function $f(x)$ is obtained.

2.2. Diffraction Limit in Holographic Imaging

There are physical factors such as the angle subtended by the scanned aperture, the antenna solid angle, and the signal to noise ratio (SNR) that can reduce the useful span in k-space (upper bounds for k_x). The optimal choice of the upper bound $k_x^{\max}$ is a compromise between the spatial resolution (better with larger bound) and the suppression of the high spatial-frequency noise (better with smaller bound). In practice, proper bound is usually employed together with spectral filtering in order to deal with noise.

As shown in Fig. 1(b), we assume that the antenna performs the scan on a line placed at the far-field of the object. In such case, the spectrum of the measured waves by the antenna over the scanned line corresponds to only the propagating wave spectrum. This implies that k_x is not larger than the following limit [8]:

$$k_x^{\max} \approx 2k \sin(\frac{\theta_b}{2}) \tag{5}$$

where θ_b is the lesser of the full beamwidth of the antenna or the angle subtended by the aperture. In the limit when the full beamwidth of the antenna is very large and for large apertures $k_x^{\max}$ moves toward $2k$ and the resolution tends to $\lambda_b/4$, where λ_b is the wavelength in the background medium. This is the diffraction limit in the resolution for far-field imaging. For imaging of sources (instead of objects) this limit is $\lambda_b/2$ (due to the path between the antenna and the source traveled once as opposed to an object for which this path is traveled twice).

2.3. Sub-Diffraction Imaging with Near-Field Scatterers

Here, we propose using a resonant scatterer moving with the antenna but in the near-field zone of the objects to achieve sub-diffraction resolution (as shown in Fig. 1(b)). In the near-field of the object, there are strong evanescent wave components that contain information corresponding to the sub-diffraction details of the object. These strong components generate currents on a scatterer placed in the near-field zone. These currents, in turn, produce secondary scattered components part of which reaches the antenna in the form of propagating waves. This secondary propagating spectrum can be measured by the antenna along with the propagating spectrum due to the primary scattered waves generated by the object. Thus, a portion of the information related to evanescent spectrum of the primary scattered waves due to the object is restored and measured by the antenna in the far-field.

3. HOLOGRAPHIC IMAGING WITH STATIONARY ANTENNA AND MOVING SCATTERER

The concept of using a scatterer in the holographic imaging to overcome the diffraction limit in the resolution can be employed for another useful holographic imaging configuration. In this configuration, as illustrated in Fig. 2, the antenna is stationary while the scatterer performs the scan along a line in the near-field zone of the object. Having the antenna stationary may be useful in many applications, for example: i) when the antenna and the measurement system are bulky and it is not easy or practical to perform the scanning by the antenna, ii) in microwave imaging applications where the movement of the connecting cables may produce additional noise or uncertainty in the measurement system or iii) in the remote sensing or underground imaging applications where moving the antenna by a plane or drone is costly.

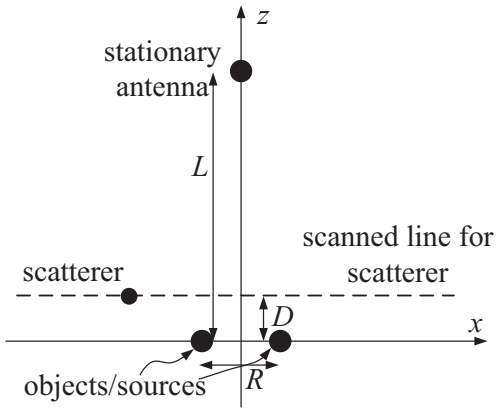

Figure 2. Illustration of the holographic imaging with stationary antenna and moving scatterer.

To implement holographic imaging in this configuration, similar to the case of moving antenna, the measured responses without the presence of the objects are subtracted from the measured responses in the presence of the objects (over the same scanned aperture) to produce the calibrated scattered responses $E_j^{\mathrm{sc,co}}(x)$ and $E_j^{\mathrm{sc}}(x)$. Then, the image reconstruction process is similar to the previous section.

4. RESULTS

In this section, we study the effect of scatterers on the resolution of holographic imaging. For this purpose, we employ FEKO software [9] which is a high-frequency simulation software based on the method of moments (MoM). All simulations are performed assuming air background with the operation frequency of 1 GHz. The scanned linear apertures for the antenna and the scatterer(s) in all simulation examples are 10λ long and centered at $x = 0$. The antenna is a y-polarized half-wavelength dipole scanning along $z = \lambda$ line. Also, for implementing the holographic imaging, in all examples, PSF, i.e., $E_j^{\mathrm{sc,co}}(x)$ in (2) is obtained approximately by scanning a CO which is a PEC sphere with diameter of $\lambda/40$. Although here we focus on the one-dimensional (1D) imaging, the outcome of this study can be extended to two-dimensional (2D) imaging.

First, we study the effect of the distance between the scanned linear aperture for the scatterer and the object (D in Fig. 1(b)). The scatterer is a half-wavelength wire along the y axis. The imaged objects are two PEC spheres with diameter of $\lambda/40$ and center-to-center distance of $R = 0.18\lambda$. Fig. 3(a) shows the reconstructed images without using scatterer as well as when using scatterer and with decreasing D from $\lambda/10$ to $\lambda/30$. Significant improvement in the resolution is observed with decreasing D. Also, Fig. 3 shows that the accuracy of object localization along the x axis degrades slightly with decreasing D. Fig. 3(b) shows the results for a similar example but with the scatterer being a quarter-wavelength.

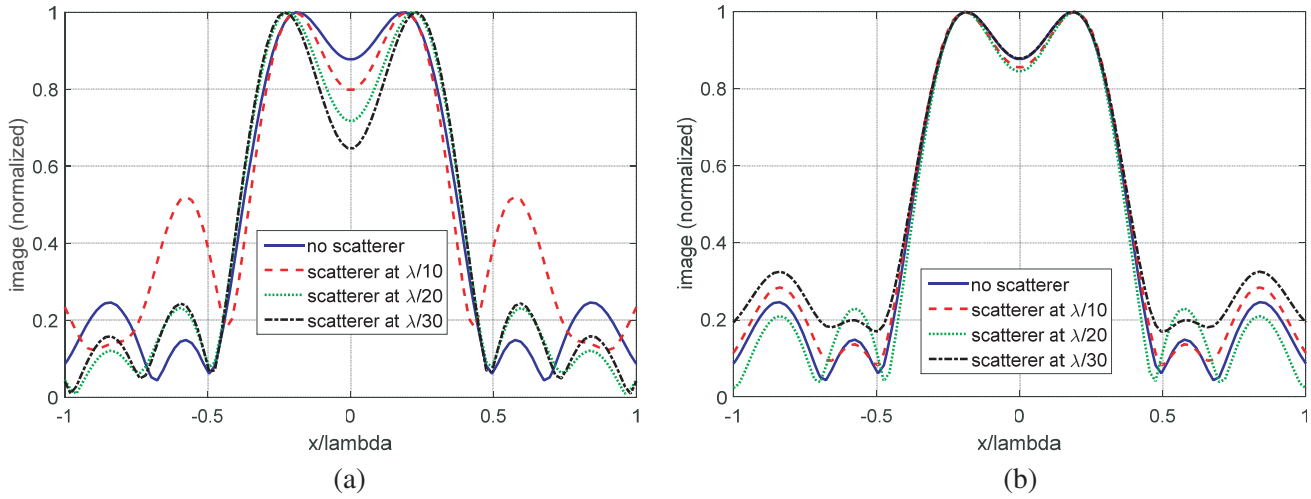

Figure 3. (a) Images when changing D in Fig. 1(b) with resonant scatterer. (b) Images when changing D in Fig. 1(b) with non-resonant scatterer.

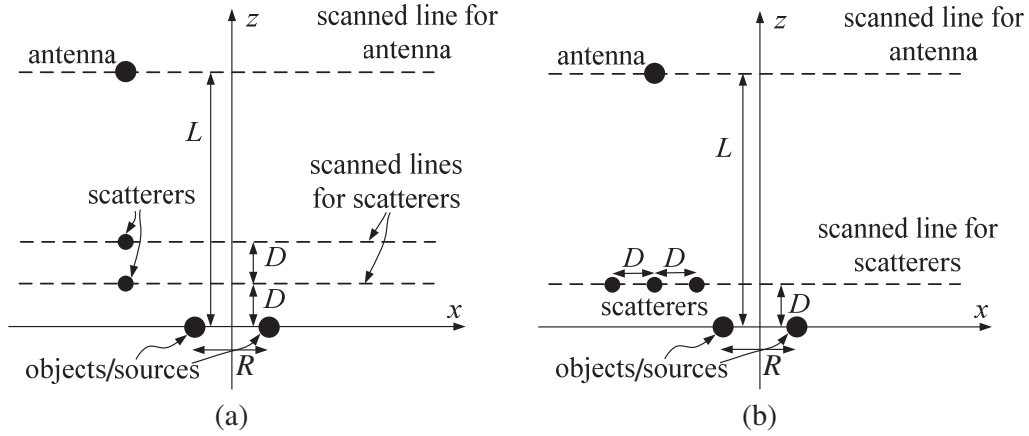

Figure 4. (a) Using two scatterers along the z axis (with $D = \lambda/20$). (b) Using three scatterers along the x axis (with $D = \lambda/20$).

It is observed that this non-resonant scatterer does not improve the resolution as much as the resonant scatterer in Fig. 3(a).

Next, we study the effect of having two scatterers aligned along the z axis and moving together with the antenna as shown in Fig. 4(a). Fig. 5(a) shows the images for this configuration compared with the cases when using a single scatterer or no scatterer. It is observed that when using two scatterers along the z axis, the resolution is improved significantly compared with the use of one scatterer. Further improvement in the resolution in this example indicates that a portion the evanescent spectrum for the secondary scattered wave due to the scatterer is also converted to propagating wave which is measured by the antenna. However, similar to the results shown in Fig. 3, the accuracy of the object localization along the x axis degrades slightly with improving the resolution.

Figure 4(b) shows the imaging configuration for the next test in which three scatterers are aligned along the x axis and they move together with the antenna. Fig. 5(b) shows the reconstructed images with these three scatterers as well as for the cases that only one scatterer or no scatterer is used. It is observed that, in contrast to the previous example (adding additional scatterer along the z axis), adding scatterer along the x axis does not improve the resolution.

In the last imaging test, the technique proposed in Section 3 is examined. For this purpose, two

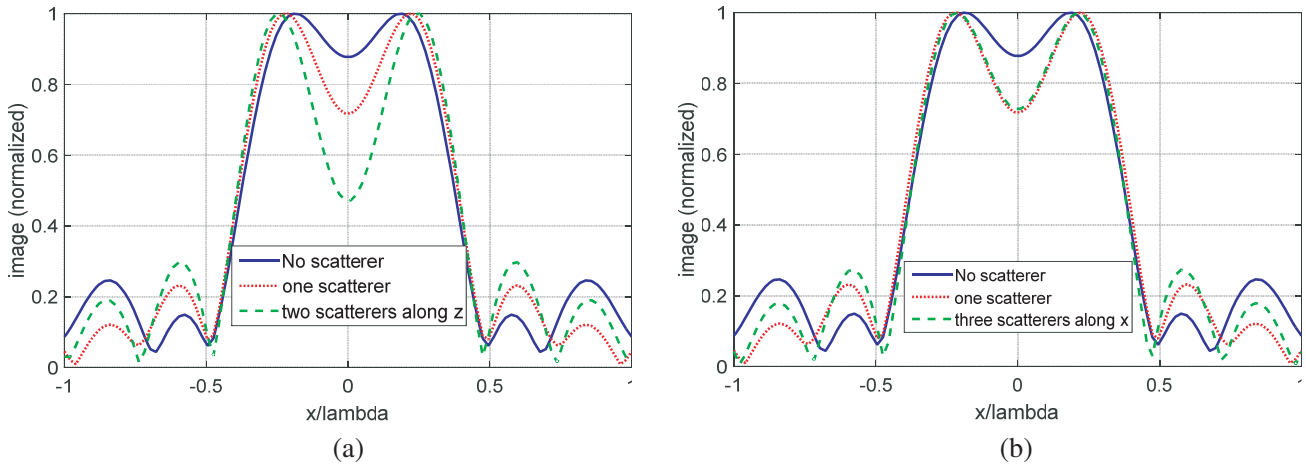

Figure 5. (a) Improvement in the resolution when using two scatterers along the z axis. (b) Almost no change in the resolution when using three scatterers along the x axis.

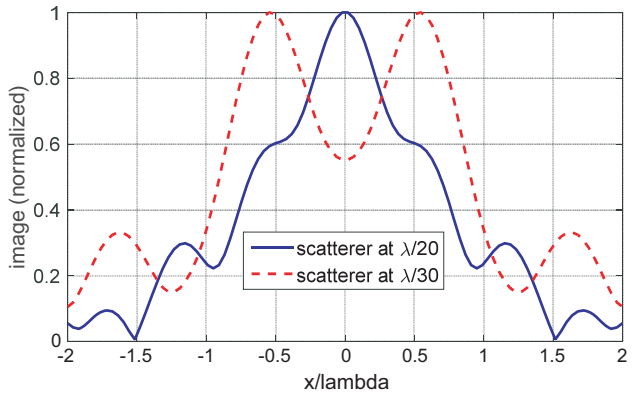

Figure 6. Reconstructed images when the antenna is stationary and the scatterer scans over a line in the near-field of the object.

PEC spheres with diameter of $\lambda/40$ and center-to-center distance of $R = 0.35\lambda$ are imaged when the antenna is stationary at $x = 0$ and $z = \lambda$ and the scatterer scans the object at a distance D. Fig. 6 shows the reconstructed images when D is $\lambda/20$ and $\lambda/30$. It is observed that deceasing D improves the resolution significantly.

5. CONCLUSIONS

We proposed a technique to overcome the well-known diffraction limit in the resolution for the holographic imaging. In this technique, although the antenna performs scanning at the far-field of the imaged objects, a resonant scatterer is moving together with the antenna but in the near-field zone of the object. We studied the improvement in the resolution as the scatterer-object distance decreases. We also showed that using more scatterers along the range direction (z axis) further improves the resolution while using more scatterers along the cross-range direction (x axis) does not improve the resolution significantly. Besides, an imaging scenario was proposed based on a stationary antenna in the far-field and a scanning scatterer in the near-field. Here, the proof-of-concept examples were shown with simulation software. In the next step, we proceed with constructing an experimental setup in which modulated scatterer technique (MST) [10] will be employed to detect the small change in the measured response due to the presence of the scatterer in the near-field of the object.

REFERENCES

1. Pendry, J. B., "Negative refraction makes a perfect lens," *Phys. Rev. Lett.*, Vol. 85, No. 18, 3966–3969, Oct. 2000.
2. Grbic, A. and G. V. Eleftheriades, "Overcoming the diffraction limit with a planar left-handed transmission-line lens," *Phys. Rev. Lett.*, Vol. 92, No. 11, 117403–117401, Mar. 2004.
3. Grbic, A., L. Jiang, and R. Merlin, "Near-field plates: Subdiffraction focusing with patterned surfaces," *Science*, Vol. 320, No. 5875, 511–513, Apr. 2008.
4. Markley, L. and G. V. Eleftheriades, "Meta-screens and near-field antenna-arrays: A new perspective on subwavelength focusing and imaging," *Metamaterials*, Vol. 5, No. 2–3, 97–106, Elsevier, Jun.–Sep. 2011.
5. Amineh, R. K. and G. V. Eleftheriades, "2D and 3D sub-diffraction source imaging with a superoscillatory filter," *Optics Express*, Vol. 21, No. 7, 8142–8157, Mar. 2013, http://dx.doi.org/10.1364/OE.21.008142.
6. Malyuskin, O. and V. Fusco, "Far field subwavelength source resolution using phase conjugating lens assisted with evanescent-to-propagating spectrum conversion," *IEEE Trans. Antennas Propag.*, Vol. 58, No. 2, 459–468, Feb. 2010.
7. Amineh, R. K., J. McCombe, A. Khalatpour, and N. K. Nikolova, "Microwave holography using point-spread functions measured with calibration objects," *IEEE Trans. Instrumentation and Measurement*, Vol. 64, No. 2, 403–417, Feb. 2015.
8. Sheen, D. M., D. L. McMakin, and T. E. Hall, "Three-dimensional millimeter-wave imaging for concealed weapon detection," *IEEE Trans. Microwave Theory Tech.*, Vol. 49, No. 9, 1581–1592, Sep. 2001.
9. FEKO, HyperWorks 14.0, http://www.altairuniversity.com/academic/.
10. Bolomey, J. C. and F. E. Gardiol, *Engineering Applications of the Modulated Scattering Technique*, Artech House Publishers, 2001.